THE MOLECULAR IMPACT OF

INTERFERON REGULATORY FACTOR 2 BINDING PROTEIN-LIKE MUTATIONS IN

NEURODEVELOPMENTAL DISORDER WITH REGRESSION, ABNORMAL MOVEMENT, LOSS OF SPEECH, AND SEIZURES

by

Sarah Aiden Bauer

A thesis submitted to the Faculty of the University of Delaware in partial fulfillment of the requirements for the degree of Master of Science in Biological Sciences

Spring 2025

THE MOLECULAR IMPACT OF

INTERFERON REGULATORY FACTOR 2 BINDING PROTEIN-LIKE MUTATIONS IN

NEURODEVELOPMENTAL DISORDER WITH REGRESSION, ABNORMAL MOVEMENT, LOSS OF SPEECH, AND SEIZURES

by

Sarah Aiden Bauer

Approved: _____
Matthew E. R. Butchbach, Ph.D.
Professor in charge of thesis on behalf of the Advisory Committee

Approved: _____
Velia M. Fowler, Ph.D.
Chair of the Department of Biological Sciences

Approved: _____
Caleb Everett, Ph.D.
Interim Dean of the College of Arts and Sciences

Approved: _____
Louis F. Rossi, Ph.D.
Vice Provost for Graduate and Professional Education and
Dean of the Graduate College

ACKNOWLEDGMENTS

I would like to thank my advisor Dr. Matthew E.R. Butchbach for providing guidance and wisdom that will follow me through life, and for helping me understand the kind of scientist I hope to be.

Thank you to my committee members Dr. Rodney Scott, Dr. Molly Sutherland, Dr. Lisha Shao, and Dr. Jeffrey Mugridge for supporting me, challenging me, and reminding me I'm not as dumb as I think I am.

A special thank you to Dr. Erica Selva and Dr. Molly Sutherland for helping me navigate the many twists, turns, and catastrophes of graduate school.

Thank you to the University of Delaware BioImaging Center, especially Dr. Sylvain Le Marchand whose guidance regarding imaging and data processing proved invaluable. Microscopy access at the University of Delaware BioImaging Center is supported by grants from the National Institute of General Medical Sciences (P20 GM103446 and P20 GM139760) and the State of Delaware. The Zeiss LSM880 confocal microscope was acquired by a shared instrumentation grant from the National Institutes of Health (S10 OD030321)

This degree would not have been completed without the support of Ricki and Gamma, who provided emotional support and could probably tell you just as much about this project as I could.

Thank you to all the previous members of the MNDRL group. In particular, Miho wrote amazing protocols, Maya kept the ship afloat, and Josh reached high shelves. Special designation to Olivia for being the only other student in the lab as well as the nicer half of the brain cell.

I am incredibly grateful for the friends I've made during my time in Delaware. To Elise, Bailey, Emily, Johnny, and Kate, here's hoping that we continue to support each other in the future as we have done through school.

Thank you to My Fiancé Nate for supporting my dreams, listening to all the ranting, and doing a lot of driving.

And most importantly, thank you to my sisters for being the best parents I could have asked for. Without your continued support, I would not be the person I am today, and I never would have achieved this many of my goals.

TABLE OF CONTENTS

LIST OF TABLES

LIST OF FIGURES

ABSTRACT

One out of every six children globally will be diagnosed with a neurological disorder before age 14. Degenerative disorders specifically have a large impact as they can affect patients for decades following diagnosis. Neurodevelopmental disorder with regression, abnormal movements, loss of speech, and seizures (NEDAMSS) is an early-onset neurodegenerative disease that is characterized by *de novo* loss of function mutations in *Interferon Regulatory Factor 2 Binding Protein Like* (IRF2BPL). NEDAMSS patients experience regression and eventual loss of motor function/control, loss of speech, and seizures. As of 2024, there have only been 65 NEDAMSS patients identified. Like many other childhood neurodegenerative diseases, there is very little known about the mechanism underlying disease progression in these patients. As such, there are currently no treatment options for children with NEDAMSS outside of mediating the symptoms as they appear.

IRF2BPL is a nuclear protein that is predominately expressed in neuronal tissue. Previous studies have demonstrated links between the E3 ubiquitin ligase activity of *IRF2BPL* and modulation of androgen receptor (AR) as well as WNT signaling. Our goal in this project is to characterize the molecular phenotype present in NEDAMSS patient cells. We observed an increase in the expression of IRF2BPL in healthy and NEDAMSS cells at both the protein and RNA levels and confirmed a

method to reprogram fibroblasts into motor neurons. Using confocal imaging, we were able to establish that IRF2BPL is being mislocalized to the cytoplasm in cell lines carrying various mutations in IRF2BPL. The misregulation of WNT signaling in NEDMASS disease progression was further explained to involve the misregulation of *LEF1 and JAGGED1*. Additionally, a reduction of *RAB25* seen in patient cells gives credence to the theory that AR signaling may play a role in developing the NEDAMSS phenotype.

Chapter 1
INTRODUCTION

1.1 Children's Motor Neuron Diseases and NEDAMSS

Children and the elderly are the two populations that are most severely impacted by neurological diseases (Steinmetz et al., 2024). Motor neuron diseases (MND) are a subclass of neurological diseases characterized by changes in motor function and/or damage in motor neurons in the brain and spinal cord (Teoh et al., 2017) . MNDs impact Motor neurons, which are polarized cholinergic cells found in the brain and spinal cord(de Carvalho and Swash, 2023). Motor neuron diseases (MND) are a subclass of neurological diseases characterized by changes in motor function and/or damage in motor neurons in the brain and spinal cord (Teoh et al., 2017). The most well-known MND seen in children is spinal muscular atrophy (SMA). This is a debilitating disease that affects 1 in 10,000 births globally (Lally et al., 2017) and until recently was untreatable (Butchbach et al., 2010). Neurodevelopmental disorder with regression, abnormal movement, loss of speech, and seizures (NEDAMSS) is an ultra-rare childhood neurological disease characterized by mutations in *interferon regulatory factor 2 binding protein-like (IRF2BPL)* and the focus of this study. This disease was first identified in 2018 (Tran Mau-Them et al., 2019) and recorded in less than 100 patients as of 2024

(Venkateswaran et al., 2024). Children with NEDAMSS will reach common developmental milestones followed by a period of regression. Typically, patients are first identified when they are brought in for seizures or sudden falling spells. Once more common diseases are ruled out, these children and their families usually undergo whole exome or whole genome sequencing as it is currently the best way to test for NEDMASS. There are also no current treatment options outside of treating the symptoms as they appear, such as prescribing anti-convulsant medications for seizures, providing mobility aids for walking and falling, and eventually life support measures. Even with the best available interventions, the regression will continue until the child is unable to walk, stand, or speak. In many cases, the children will be wheelchair-bound and unable to breathe on their own.

1.2 IRF2BPL Localization and Possible Functions

IRF2BPL is a nuclear protein that is predominately expressed in neural tissue. All known NEDAMSS cases thus far have been marked by *de novo* mutations in *IRF2BPL*. NEDAMSS-linked mutations in *IRF2BPL* occur throughout the protein (Figure 1), indicating there is not one specific region within the gene that is linked to the disease state. Previous studies have looked more in-depth at the various regions of the gene and whether the loss of a particular region would lead to the same phenotype as NEDAMSS mutations (Marcogliese et al., 2022). They found that the individual deletion of the Really Interesting New Gene (RING) domain located at the C terminus,

which contains a zinc finger and is involved in protein-protein interaction as well as the ubiquitination pathway. the DNA binding domain located near the second zinc finger at the N terminus, and the nuclear localization domain did not recapitulate the NEDAMSS phenotype.IRF2BPL contains two coiled-coil domains that help with protein-protein interaction and cell division. There are several PolyA domains that regulate RNA binding as well as several PolyQ domains that are linked with neurological diseases such as Huntington's. In a study done in fruit flies, it was noted that a complete knockout of *pits* (the fly ortholog of IRF2BPL) is homozygous lethal (Marcogliese et al., 2022).

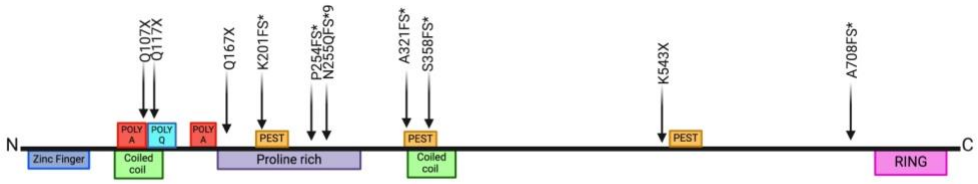

Figure 1: Mutation Map of IRF2BPL

Protein map with structures and patient mutations.
Patient sex, mutation location, and control lines are listed in Table 1. Created with BioRender.com

Heterozygous *pits* knock-out flies show a motor deficit in climbing assays. Additionally, zebrafish with a heterozygous or homozygous knockout of IRF2BPL showed a similar motor deficiency in swimming speed (Marcogliese et al., 2022). These observations support the involvement of motor neurons in this disease.

The native function of IRF2BPL remains unknown making understanding the impact of its dysregulation difficult. It has recently been theorized to act as an E3 ubiquitin ligase (Higashimori et al., 2018). The ubiquitin-proteasome system (UPS) works alongside autophagy to ensure that misfolded or damaged proteins are properly degraded and removed from cells. The UPS is thought to be responsible for the degradation of up to 80% of proteins. As part of the three-step UPS cascade, E3 ubiquitin ligases act to bind to the E2- UB conjugated complex and help transfer it to its target (Yang et al., 2021). Dysfunction of the E3 ligases has been linked with cancer progression as well several neurological disorders including Angelman syndrome which shares phenotypic similarities with NEDAMSS (Köhler et al., 2017; Lescouzères and Bomont, 2020).

1.3 WNT and AR Signaling In Relation to NEDAMSS

WNT signaling is a well-known signaling pathway present in most vertebrates. WNT signaling is involved in modulating gene expression, cell polarity, cell differentiation, and proliferation (Oliva et al., 2018). WNT signaling is disturbed in many diseases, including cancers and neurological diseases such as amyotrophic lateral sclerosis (ALS) in ALS WNT signaling is thought to increase the degradation of motor neurons by increasing glial cell activity, decreasing cell survivability and damaging the neuromuscular junction (Jiang et al., 2021; Ng et al., 2019; Soumya et al., 2023). In the activated β-catenin dependent WNT signaling pathway β-catenin is transported

into the nucleus and binds with *LEF1* before binding to the DNA. In the inactive stateβ-catenin is bound to a destruction complex and broken down before it can interact with DNA.

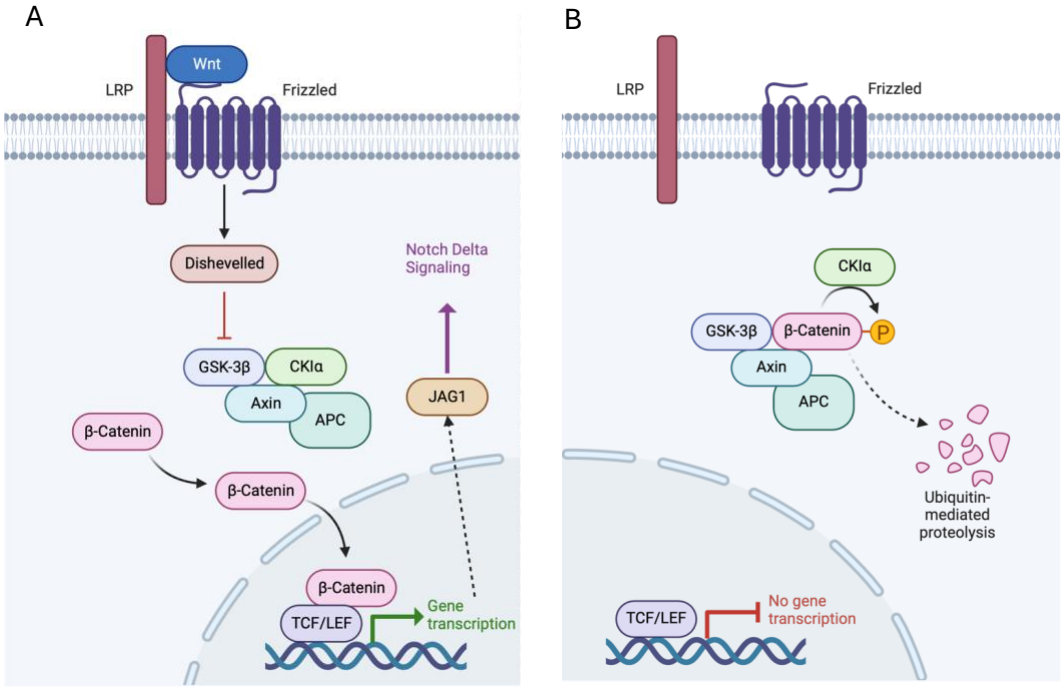

Figure 2: Model of Canonical WNT Signaling Pathway.

A) Canonical Activated WNT Signaling pathway B) Canonical Inhibited WNT Signaling pathway. Created with BioRender.com

In a 2022 study, the loss of IRF2BPL ortholog in fruit flies showed an increase in WNT1 protein as well as RNA, indicating that this excess of WNT signaling may be responsible for the observed neurological and physical phenotype (Marcogliese et al., 2022). That same study showed a progressive loss of functional axons in the *pits* flies as they aged, correlating with neurological degeneration, which mimics the progressive cerebral atrophy observed in NEDAMSS patients (Marcogliese et al., 2018).

EAP1 (the rat ortholog of IRF2BPL) has been identified as a modulator of androgen receptor signaling in cancer pathogenesis (Yokoyama et al., 2021). Like WNT signaling, AR signaling is a well-established and important cell signaling process, mostly associated with male sexual development as well as cell growth and muscle development. Specifically AR signaling has been shown has being very impactful in motor neuron viability and breakdown(Cary and La Spada, 2008) Several studies have been conducted to clarify which proteins naturally interact with AR (Chen et al., 2022) this analysis using has repeatedly shown IRF2BPL to be one of the more prominent candidates. As IRF2BPL is theorized to function as an E3 ubiquitin ligase, it may be involved in the activation and subsequent degradation of AR in the signaling cascade(Li et al., 2014).

There is a large amount of evidence for overlap and interaction between AR signaling and WNT Signaling. Modulation or absence of AR signaling has been shown to increase the levels of β-catenin present in cells, suggesting that AR may be a negative regulator of WNT signaling (Kretzschmar et al., 2015). AR-negative cancer cells have also shown increased WNT activity (Wan et al., 2012). Given the previously reported changes in WNT signaling in NEDAMSS and the deep-seated connection between WNT signaling and AR signaling exploration of AR signaling in this disease is a logical choice.

LEF1 and JAG1, two common components of the WNT signaling pathway, are also involved in AR signaling. JAG1 is a downstream marker for WNT signaling that acts as a ligand for notch delta receptor binding. Recently, JAG1 was shown to increase

AR expression and activity in prostate cancer (Tran and Lee, 2022). LEF1 acts as a transcription factor binding to β-catenin in WNT signaling to facilitate gene expression and may be a key regulator in AR signaling as it binds to the AR promotor gene (Akiyama, 2000; Lutterbach and Hiebert, 2000) If WNT or AR signaling is playing a key role in NEDAMSS disease progression, this could provide a possible target for future treatments. Several small molecules can modulate both AR and WNT cascades(Loddick et al., 2013; Tran and Zheng, 2017). Given that many of these compounds have already been identified, the testing and move to clinical research could be expedited.

1.4 Modeling Pediatric Neurological Diseases

It is difficult to investigate neuronal diseases such as NEDAMSS due to poor access to affect neurons in these patients. Luckily, these problems are usually avoided by using model organisms. Many different types of animal models can be used, from worms to pigs. Typically, neurological models are in mice or rats as they are closer to humans in phenotypic presentation than other animals, and they are a more cost-efficient option compared to primates or pigs. Regardless of the model organism, it is exceedingly difficult to completely recapitulate the human disease due to the basic fact that they are not identical to humans.

One of the more recent solutions to this difficulty recapitulating human disease in an animal model has been to use induced pluripotent stem cells (iPSCs). This approach

allows researchers to convey already differentiated cells with a few genes and return them to a pre-differentiation state similar to that of embryonic stem cells that can then be differentiated into whatever cell type is needed (Takahashi and Yamanaka, 2006). This method moves past many limitations associated with animal models but is not without its own limitations. In the process of converting differentiated cells, such as dermal fibroblasts, into iPSCs and then into the cell type of interest, valuable information that is unique to each patient is lost. Epigenetics has been shown to play an important role in gene expression and disease progression (Liu et al., 2016).

Direct reprogramming offers a way to take patient or healthy cells and directly convert them into motor neurons, or astrocytes, without losing the epigenetic information. Epigenetics is the study of how your environment and experiences can impact gene expression. This is important clinically as it can factor into whether people with the same genetic information do or do not present with the disease phenotype (Dupont et al., 2009). Current research suggests that some diseases may be triggered by the environment during development and would have remained neutral without outside interference (Aas et al., 2016).

By using lentiviral delivery of neurotrophic factors (Figure 3), such as *NGN2*, a neuronal pioneer factor that acts to open chromatin for motor neuron-specific genes such as *SOX11*, *ISL1*, and *LHX3*. Using direct reprogramming could provide a vital resource for studies concerning poorly characterized diseases where human samples are not available, and animal models are not sufficient.

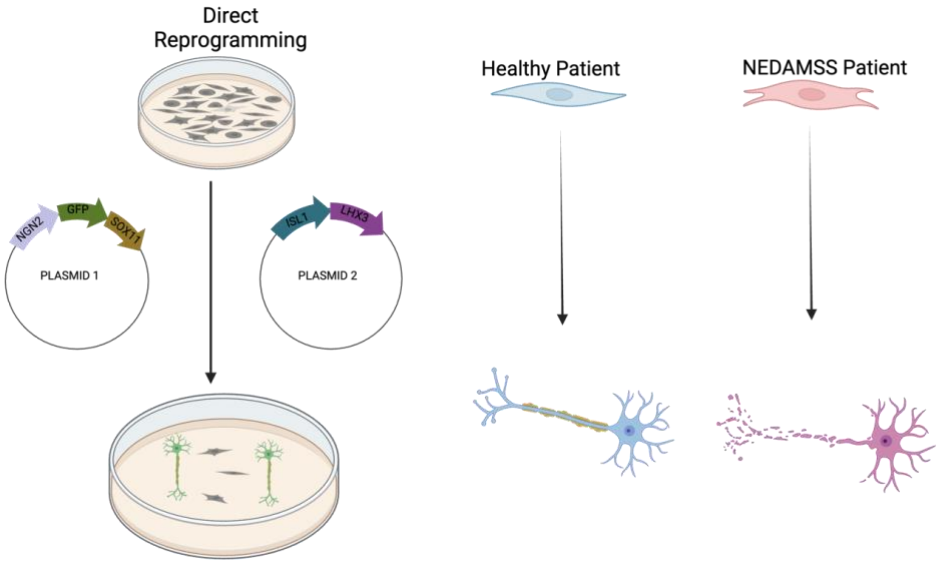

Figure 3: Overview of Direct Reprogramming of Fibroblasts into Motor Neurons

Graphic depiction of Direct Reprogramming including plasmid map of neurotrophic factors which will be used to reprogram fibroblasts. Plasmid 1: pCSC-NGN2-IRES-GFP-T2A-Sox11. Plasmid 2: pCSC-ISL1-T2A-LHX3 Created with BioRender.com

1.5 Hypothesis

The goal of this project is to characterize the molecular phenotype present in NEDAMSS cells, namely fibroblasts and motor neurons. In this study, we examined whether the mislocalization and abnormal expression of IRF2BPL shown in previous studies using nonvertebrate model systems is similar in human fibroblast samples. We found that NEDAMSS patient cells had mislocalization of IRF2BPL to the cytoplasm as well as an increase in expression when compared to healthy age/sex-matched controls. We further characterized molecular pathways that are impacted by NEDAMSS pathogenesis (Figure 4). There is no published theory on the mechanism of IRF2BPL impacting AR signaling yet. We focused further on the impact these mutations would have on motor neurons in an effort to clarify the pathology of motor dysfunction in this disease.

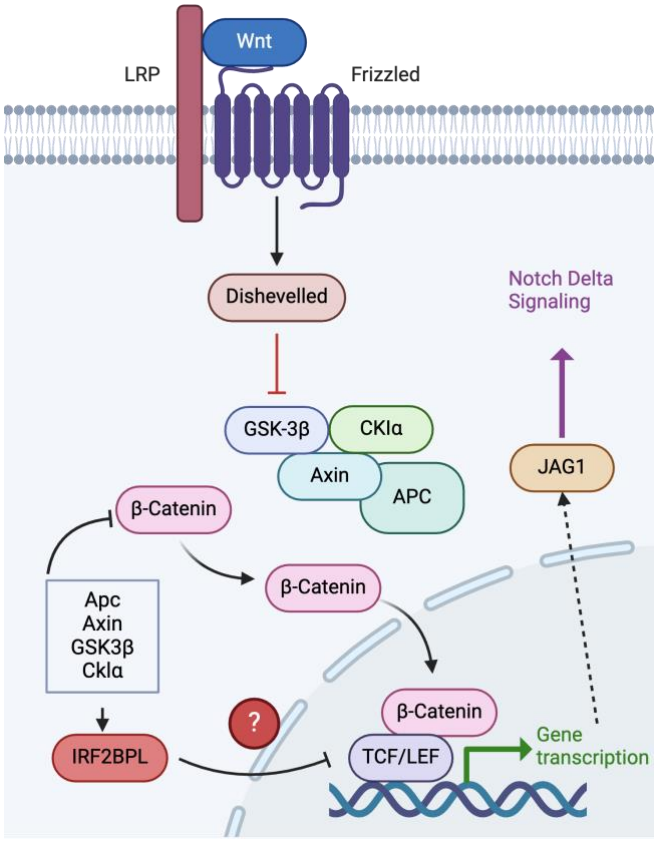

Figure 4 Proposed Mechanism of IRF2BPL Regulation of WNT Signaling. This figure is adapted from (Marcogliese et al., 2022).

Chapter 2
MATERIALS AND METHODS

2.1 Fibroblast Cell Culture

Patient fibroblast cell lines were derived from skin biopsies derived from NEDAMSS patients containing different mutations (n=10) in *IRF2BPL* (**Table 1**). These NEDAMSS cell lines were provided by Dr. Pawel Lisowski (Charité – Universitätsmedizin Berlin, Germany). Control fibroblast cell lines were derived from sex-matched healthy samples established by the Motor Neuron Diseases Research Lab. Fibroblast lines were maintained in Dulbecco's Modified Eagle Medium (DMEM; Life Technologies, Grand Island, NY) with 10% fetal bovine serum (Equal Fetal; Atlas Biologicals, Fort Collins, CO), 2mM L-glutamine (Life Technologies), and 1% penicillin/streptomycin solution (Life Technologies). Cells were grown in a humidified incubator with 5% CO_2 at 37ºC.

Table 1: Patient Cell Lines with Mutations

NEDAMSS CELL LINE	SEX	IRF2BPL RNA Mutation	IRF2BPL Protein Mutation
601	F	??	p.P254fs*
GCD00082	F	c.1627A>T c.349C>T	p.K543X p.Q117X
LPOW187	F	c.499C>T	p.Q167X
NW	F	c.319C>T	p.Q107X
P28712	F	c.962del	p.A321fs*
DR	M	c.319C>T	p.Q107X
PT	M	c.603delA	p.K201fs*
TEO	M	c.1074-1075del	p.S358fs*
UKE672479	M	c.762dupC	p.N255Qfs*9
ZKW645	M	c.2122delG	p.A708fs*

2.2 qRT-PCR

Total RNA was isolated from cell pellets utilizing the RNeasy Mini Kit (QIAGEN, Germantown, MD) following the instructions from the manufacturer. cDNA was prepared from 0.25 to 0.5 ug RNA using the iScript™ cDNA Synthesis Kit (Bio-Rad, Hercules, CA, USA). Target transcripts were amplified via PCR from cDNA diluted

200–400-fold using the QuantiTect SYBR Green PCR kit (QIAGEN). The primer sets listed (Integrated DNA Technologies; Coralville, IA) (Table 2) for the target transcripts were used. The relative transcript levels were calculated using the efficiency-adjusted $2^{-\Delta\Delta Ct}$ method (Schmittgen and Livak, 2008; Yuan et al., 2008). The primer efficiency (E) for each primer set was calculated from the slope of a C_t versus $\log_{10}$(cDNA serial dilution) curve ($E = 10^{[-1/slope]}$)(Pfaffl, 2001). ΔC_t, adjusted, is the difference between the adjusted C_t (C_t, measured × E) for the target transcript and the geometric mean of the adjusted C_t values for the three reference genes (Vandesompele et al., 2002). $\Delta\Delta$ C_t is defined as the difference between the Δ C_t for the NEDAMSS sample and the Δ C_t for the control sample. The reference transcripts were *ACTB, RPLP0,* and *GAPDH.*

Table 2: qPCR Primers and Primer Efficiencies

Primer Target	Sequence	qPCR Efficiency	Efficiency Factor
ACHE	Fwd: cattcccagaagtcccagaag Rev:cagacaaagagccagagagatg	113.9735502	1.139735502
ACTB	Fwd: gaagtcccttgccatcctaaa Rev: gctatcacctcccctgtgtg	101.7	1.017
AR	Fwd: cttcccattgtggctcctatc Rev: ctctaaacttcccgtggcataa	110.9862802	1.109862802
BACH2	Fwd: cagctctgctcttcctattc Rev: tcactggagttggttccataag	113.2520792	1.132520792
CTNNB1	Fwd:ccacaagattacaagaaacggc Rev:accagagtgaaaagaacgatagc	151.38	1.5138
GAPDH	Fwd: aatcccatcaccatcttcca Rev: aaatgagccccagccttc	94.58	0.9458
IRF2BPL	Fwd: cctctgctgcaccattt Rev: gggccttgatactctctcta	97.8759	0.978759
JAG1	Fwd: ggtaggagaggcgattgattt Rev:tcagggtggagacttgtttatg	103.8228384	1.038228384
KLK4	Fwd:gaagaaagggagggacaaagag Rev: cagacacacacacgcatact	133.1707629	1.331707629
LEF1	Fwd: gtcaactccaaagaaggcatg Rev: agtgaggatgggtagggt	79.73	0.7973
P21	Fwd: gtcactgtcttgtacccttgt Rev: gcttcctcttggagaagatcag	184.7629475	1.847629475
P27	Fwd:ctcgactcagacgtggataaag Rev: caggccatgacatctgtatttg	102.6991863	1.026991863

RAB25	Fwd:ctgaggcttagaggcaaagtag Rev:gggtaagaggatgtgtgtgtatg	129.799989	1.29799989
RPLP0	Fwd: tcatcaacgggtacaaacga Rev: agatggatcagccaagaagg	100.02	1.0002
TGFB1	Fwd: gaactcccgacctcaagtaatc Rev:ccaggtgtaagacaagacagag	145.042474	1.45042474

2.3 Immunofluorescence and Cellular Localization

Fibroblasts were plated on etched coverslips coated with 0.1% gelatin and allowed to become confluent. The cells were then rinsed with PBS and incubated for 30 mins in a Fixative solution (2% paraformaldehyde, 50 mM sucrose, 100 mM NaH_2PO_4, 100 mM Na_2HPO_4, 400 $CaCl_2$). Cells were then blocked with 5x BLOCK (5% fetal bovine serum (FBS), 5% horse serum, .5% bovine serum albumin (fraction V), and 5% 10x block in PBS) for 1 hour. Slides were then incubated overnight at 4°C in both primary antibodies (rabbit anti-IRF2BPL; 1:400 (Novus Biologicals) and mouse anti-Lactate Dehydrogenase (LDH); 1:5000 (Abcam) in 1x BLOCK). After washing with PBS, the slides were incubated with secondary antibody (Alexa Fluor 594 Goat Anti-Rabbit IgG 1:500 (Life Technologies)and Alexa Fluor488 Goat Anti-Mouse IgG (1:500)(Life Technologies) in 1x BLOCK) for 1 hour, after which the nuclei were counterstained with Hoechst 33342 (1 mg/mL diluted 1: 3000 (3µg/mL) in 1x BLOCK). Coverslips were washed with Phosphate buffered saline (PBS) and mounted onto glass slides with ImmuMount (Shandon Lipshaw), dried in a dark drawer overnight, and stored in a sealed slide box at 4°C.

2.4 Direct Reprogramming

Cells were grown in a humidified incubator with 5% CO_2 at 37ºC. Patient and healthy fibroblasts were grown in T75 flasks in fibroblast maintenance media (DMEM, 10% FBS, 1% Penicillin-Streptomycin (Pen/Strep), and 1% Glutamine (Gln)). 293FT cells were grown in fibroblast media overnight. The following day, 293FT cells were split onto 10 cm plates in fibroblast maintenance media and incubated overnight. On the third day of growth, the 293FT cells were transfected with plasmid DNA previously purified (4µg pCSC-NGN2-IRES-GFPT2ASox11, 2µg pCSC-ISL-T2A-LHX3, 1µg pMD2.G, 1µg pMDLg pRRE, and 0.5µg pRSV Rev) (Dull et al., 1998; Liu et al., 2016). Cell transfection with these plasmids was completed using Lipofectamine 2000 (Invitrogen) in OPTIMEM media (Life Technologies). 293 cells were transfected for 72 hours before lentiviral collection and VivaSpin (Cytiva) purification of the lentiviral product.

Filtered lentiviral media was combined with fibroblast media and 6µg /ml polybrene. Patient and healthy fibroblasts were incubated under this LV media overnight. The following day, the media was changed to fibroblast media. At 2 days post-infection, the growth medium for the cells was changed to Neural Induction media (Base Media (DMEM: F12+HEPES(Cytiva HyClone): neurobasal media (Life Technologies), and 1% Pen/Strep (100x) 10 ml total media per plate, 0.4% N2 supplement (Life Technologies), 0.8% B27 supplement (Gibco]), 20 µM forskolin (FSK; R& D Systems), .1 µM dorsomorphin (DM) (R&D Systems), and 10ng/mL heat stable recombinant human basic fibroblast growth factor (FGF2; R&D Systems)) Coverslips

were coated with 100 µg/mL Poly-DL-ornithine, 2 µg/mL laminin, and 1.35 µg/mL GelTrex (Gibco) as previously described (Maeda et al., 2014).

After 3 days in Neural Induction media, cells were purified using Opti-Prep Density Gradient Medium (Sigma Aldrich). Opti-Prep solution was combined with Basal media (DMEM: F12+HEPES (Cytiva HyClone): Neurobasal media (Life Technologies), and 1% Pen/Strep) to generate the density gradient described in Table 3. The cell suspensions were then pipetted on top of the density gradient without disturbing the layers. Gradients were then centrifuged for 15 minutes at 800g followed by low deceleration to maintain the gradient. Based on density, neurons should be in the bottom two layers of the purified solution (Brewer and Torricelli, 2007; Katzenell et al., 2017). The top layers were removed with the layers of interest being resuspended in 5 mL of Basal media and centrifuged for 2 minutes at 200xg. This was repeated twice to thoroughly wash the cell pellets. Finally, the cells were resuspended in Motor Neuron Maturation Media (MN; DMEM: F12+HEPES: Neurobasal, 1% Pen/Strep, 0.4%N2,0.8% B27, 5mM FSK, 10ng/mL brain-derived neurotrophic factor (BDNF; R&D Systems), 10ng/mL glial-derived neurotrophic factor (GDNF; R&D Systems), 10ng/mL neurotrophin-3 (NT3; R&D Systems)). This suspension was then used to seed three wells of a 6-well plate. The cells were incubated with MN media for 3-5 days.

Table 3: OptiPrep Dilution Table.

1 set of 4 tubes for each cell 10cm plate		
Layer	**µL OptiPrep**	**µL Basal Medium**
1	173	827
2	124	876
3	99	901
4	74	926

2.5 Immunohistochemistry of Reprogrammed Cells

After being washed with PBS, cells were incubated in a fixative solution and 5x BLOCK, as described in section 2.3. Coverslips were then incubated with primary antibody (rabbit anti-HB9; 1:2000 (Abcam) and chicken anit-ChAT; 1:1000 (Neuromics) in 1x BLOCK) at 4 °C overnight. Slides were incubated with secondary antibody (Alexa Fluor 594 goat anti-rabbit IgG; 1:500 (Life Technologies) and Alexa Fluor 647 goat Anti-chicken IgG; 1:500 (Life Technologies) in 1xBLOCK) for 1 hour, after which the nuclei were counterstained with Hoechst 33342 (1 mg/mL diluted 1: 3000 (3µg/mL) in 1xBLOCK).

Coverslips were washed with PBS and mounted onto glass slides with ImmuMount (Shandon Lipshaw), dried in a dark drawer overnight, and stored in a sealed slide box at 4°C.

Fibroblasts of each cell line were treated with the same media and plating techniques as the reprogrammed cells. These cells were harvested, washed, and fixed as described above. These control coverslips were incubated with primary antibody (Rabbit anti-HB9 1:2000 (Abcam), mouse anti-TE7 1:100 (Millipore), and chicken anit-GFP 1:1000 (Millipore) in 1x BLOCK) at 4◦ overnight. Slides were incubated with secondary antibody (Alexa Fluor594 Goat Anti-Rabbit IgG 1:500 (Life Technologies), Alex flour 488 Goat Anti chicken 1:500 (Life Technologies), and Alexa Fluor647 Goat Anti-mouse 1:500 (Life Technologies) in 1x BLOCK) for 1 hour after which the nuclei were counterstained with Hoechst 33342 solution.

2.6 Immunoblot

Cell pellets were collected by growing cells in 6 well plates at 37°C with 5% CO_2 until confluent. Cells were washed with PBS at 4°C for 1 hour. Cells were then scraped and centrifuged at 10,000xg for 10 mins, after which the supernatant was discarded and the pellet stored at -80°C. Protein was isolated by lysing the cells in lysis buffer (1X PBS, 0.1% Triton-X-100) containing a proteinase inhibitor cocktail (Roche)) and sonicating the solution (Diagenode Biorupter Standard Sonicator). The protein concentration of each sample was determined using the Pierce BCA Assay KIT (Thermo Fisher

Scientific). Solutions were diluted to yield aliquots containing 15μg of protein with lysis buffer. 6x Sodium Dodecyl Sulfate (SDS) loading dye (350 mM Tris HCl pH 6.8, 10.28% SDS, 36% glycerol, 600 mM dithiothreitol (DTT), and 0.012% bromophenol blue) and 118 mM DTT were added to each aliquot. The samples were then boiled at 100°C for 10 minutes and centrifuged briefly to collect condensation. Each sample was then added to an individual lane in a 0.1% SDS 4–20% gradient polyacrylamide gel (Bio-Rad). Precisions Plus Protein Kaleidoscope ladder (BioRad) was added to the first well on each gel. The gels were run in an electrophoretic apparatus containing 1x Running Buffer (SDS-PAGE Running Buffer (25mM Tris, 3.6 mM SDS, .2M glycine;) and]then transferred onto a precut PVDF membrane (Cytiva) using a semi-dry transfer method for 30 mins in 1x Transfer Buffer (1X SDS-PAGE Running Buffer with 2% Methanol). The membranes were rinsed in ddH_2O and treated briefly with methanol. They were then incubated with PBST (PBS with 0.1% Tween-20)-based blocking buffer (5% nonfat milk and 1% bovine serum albumin (BSA) (Sigma-Aldrich) in PBS-T) overnight at 4°C PBS. The blots were then incubated with Rabbit anti-IRF2BPL (Novus Biologicals) diluted 1:400 in 0.1x PBST-based blocking buffer overnight at 4°C. The following day, the blots were rinsed with PBST and incubated with horseradish peroxidase (HRP)-conjugated anti-Rabbit IgG, (Rockland Immunochemicals for Research.) in 0.1 PBST-based blocking buffer for 1 hour, rinsed again with PBST. Protein bands were detected using the Western Sure Chemiluminescence Kit (Licor) on the C-Digit Blot Scanner (LiCor Biosciences). The blots were then probed for mouse anti-β-actin (Abcam, 1:10000 in

0.1xPBST-based blocking buffer) overnight at 4°C probed with HRP-linked anti-mouse IgG (Rockland Immunochemicals for Research).

2.7 Acquisition and Quantification of Confocal Images

Fixed and stained cell slides were imaged on the LSM880 confocal microscope (Zeiss) located in the Ammon-Pinizzotto Biopharmaceutical Innovation Center at the University of Delaware. Slides were imaged at 63X using oil immersion. The images were quantified in ImageJ using a published method (Shihan et al., 2021).

2.8 Luciferase-Based Assay of WNT Signaling Activity in Cell Culture

Patient and control fibroblasts were grown in T75 flasks as described above. Once confluent, the cells were treated with 0.25% Trypsin EDTA (Life Technologies) and seeded into a 96-well clear bottom plate. Once cells were confluent, they were transfected with plasmid DNA that had been previously purified and nano-dropped (M50 Super 8x TOPFlash 3ug/well, M51 Super 8x FOPFlash 3ug/well (add gene), pRL-TK 3ug/well (pRL-TK Vector GenBank® Accession Number AF025846)(Promega). M50 Super 8x TOPFlash and M51 Super 8x FOPFlash were gifts from Randall Moon (Addgene plasmid # 12456, 12457)(Veeman et al., 2003; Xu et al., 2018). Cells were treated with Lipofectamine 2000 (Invitrogen) in Opti-MEM media and incubated overnight. The following day, the cells were treated with fresh

Fibroblast Media. Forty-eight hours post-infection, the luminescence was measured using the Dual-Luciferase® Reporter Assay System (Promega). Data for both plasmids of interest was normalized against the pRL-TK treated cells to control for cell number.

2.9 Plasmid DNA Isolation, Purification, and Confirmation

E.coli transfected with plasmid DNA were grown overnight on LB Agar plates (LB Agar (ThermoFisher), 100 ug/mL Ampicillin (Sigma Aldrich)) upside down in a bacterial oven at 37°C. Single bacterial colonies were used to seed Falcon tubes containing 5mL LB Media (Invitrogen) treated with 100 ug/mL ampicillin. The tubes were incubated overnight in a bacterial shaker at 250 rpm at 37°C.

Chemically competent DH5α *E. coli* cells were treated with 3uL pRL-TK plasmid DNA, incubated on ice for 30 mins, heat shocked for 30 secs at 37°C, and cooled on ice for 2 minutes before being transferred to Falcon tubes and treated with SOC media (2 g Bacto-tryptone(Sigma Aldrich), 0.5 g yeast extract (Sigma Aldrich), 0.05 g NaCl (Sigma Aldrich), 2.5 mM KCl(Sigma Aldrich), 10mM $MgCl_2$ (Sigma Aldrich) and20mM glucose (Sigma Aldrich)). The transformed cells were grown overnight on LB agar plates.

E. coli colonies were then isolated and moved into Fernbach flasks containing 250 mL LB Media treated with 100 ug/mL ampicillin and incubated overnight in a bacterial shaker at 250 rpm at 37°C.

Plasmid DNA was isolated using the QIAprep Spin Maxi Kit (Qiagen). The identity and quality of plasmid DNA samples were confirmed on the Nanodrop Spectrometer (Thermo Fisher) and restriction digest (Enzymes(Hpal, HindIII,BamHI,EcoRI) and Protocols from New England Biolabs). Products of restriction digest assays were visualized using gel electrophoresis.

2.10 Statistical Analysis

Data was expressed as means ± standard errors. One-way analysis of variance (ANOVA) of the data was completed, followed by an unpaired T-Test using GraphPad Prism version 10.0.0 for MacOS, Boston, Massachusetts USA.

Chapter 3
RESULTS

3.1 IRF2BPL Protein and RNA Expression is Upregulated in Patient Fibroblasts

The NEDAMSS skin fibroblast collection comprises five male and five female samples (Table 1). To analyze any phenotype, present in the cells with mutant IRF2BPL, all experiments and data analysis were conducted on the ten patient cells and ten healthy (non-NEDAMSS) age/sex-matched fibroblast lines. Cell pellets from NEADMSS and healthy patients were analyzed for IRF2BPL protein expression (Figure 5). Being that IRF2BPL is known to be predominately expressed in neuronal tissue, the apparent absence of protein in healthy fibroblasts is expected. Due to the truncating nature of the patient mutations in this collection, the increase of IRF2BPL protein in patient cells is surprising. The only commercially available IRF2BPL antibody targets the NLS near the C-terminal end of the protein; therefore, any mutations that produce a protein that is truncated before that point would not be detected by the antibody. There is an increase in both the full-length and truncated varieties of IRF2BPL seen on both the protein and RNA levels (Figure 5B).

Figure 5: IRF2BPL protein and RNA expression is increased in NEDAMSS cells compared to sex match control cells.

A) Immunoblot for IRF2BPL using male patient and age-sex-matched control cells. B) Relative RNA expression of IRF2BPL in patients and healthy cells. A cDNA library was generated from isolated mRNA and amplified via PCR. The resulting cDNA was analyzed using qPCR to monitor the relative expression of the RNA transcripts of interest. These reactions were done in triplicate across all cell lines. This expression is relative to the geometric mean of three reference transcripts (*GAPDH, RPL0, B-Actin*). ns-p>.05,*-p≤0.05,**-p≤0.01,***-p≤0.001

3.2 IRF2BPL is Mislocalized to the Cytosol in NEDAMSS Cells

Previous studies have established that IRF2BPL is a nuclear protein but that NEDAMSS patient cells display aberrant localization of IRF2BPL (Sinha Ray et al., 2022). We confirmed this observation in this NEDAMSS cohort using immunohistochemistry and confocal microscopy (Figure 6). In a healthy male fibroblast, we see there is nuclear localization, as demonstrated by the colocalization of IRF2BPL with Hoechst 33342 (HST), which stains the DNA in the

nucleus(Magavi et al., 2000) (Figure 6A). In the cells of a male patient, we see colocalization between IRF2BPL and lactate dehydrogenase (LDH), a ubiquitously expressed enzyme commonly used as a cytosolic marker (Figure 6B).

To more precisely quantify the difference in localization between NEDAMSS and healthy cells, the mean fluorescence intensity (MFI) of the whole cell and nucleus were compared and referenced to the MFI of the background of the image to account for autofluorescence (Figure 6C) using a previously described method (Shihan et al., 2021). There is significantly more nuclear IRF2BPL in the healthy cells than in the NEDAMSS cells. These quantitative colocalization studies, along with the *IRF2BPL* expression data (Figures 5-6), confirm that IRF2BPL is indeed aberrantly localized outside of the nucleus in NEDAMSS fibroblasts.

A

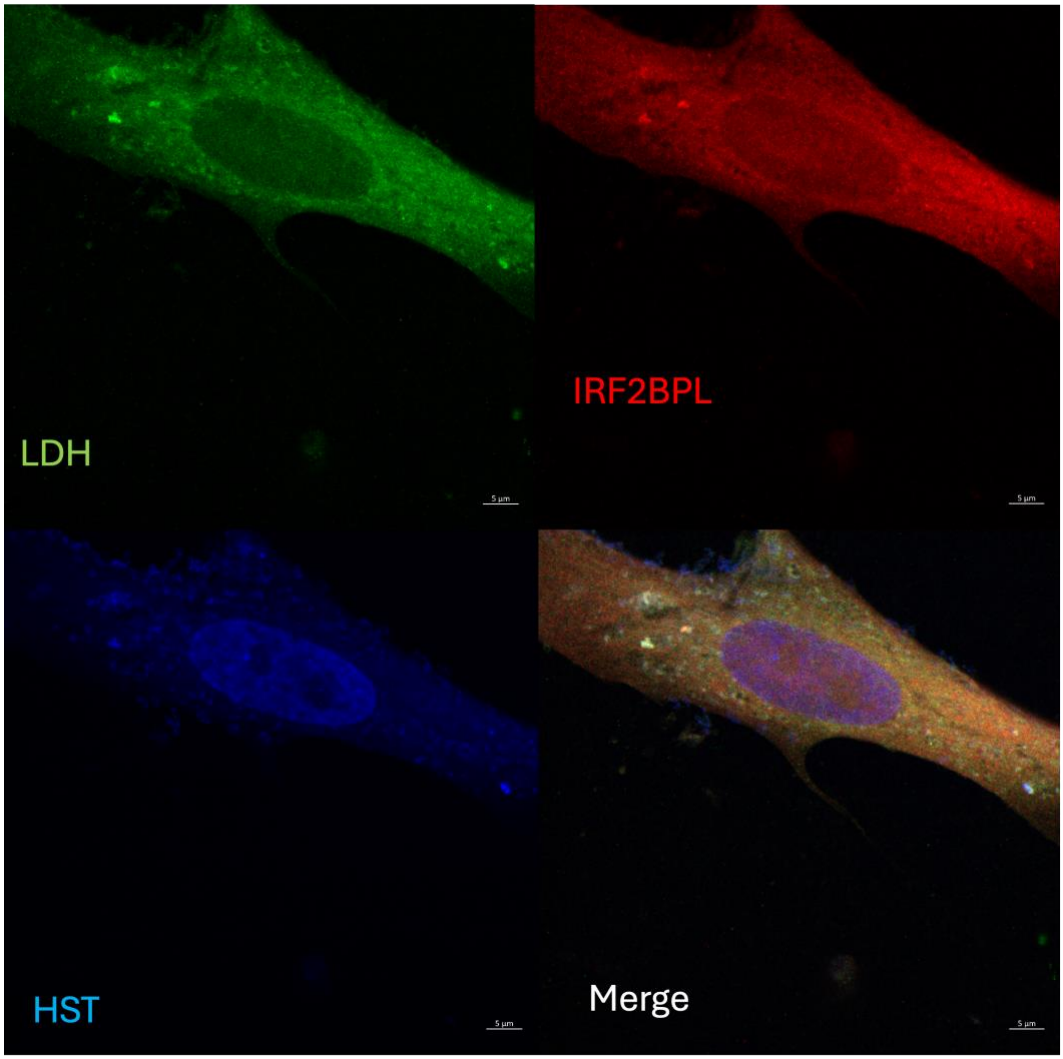

B

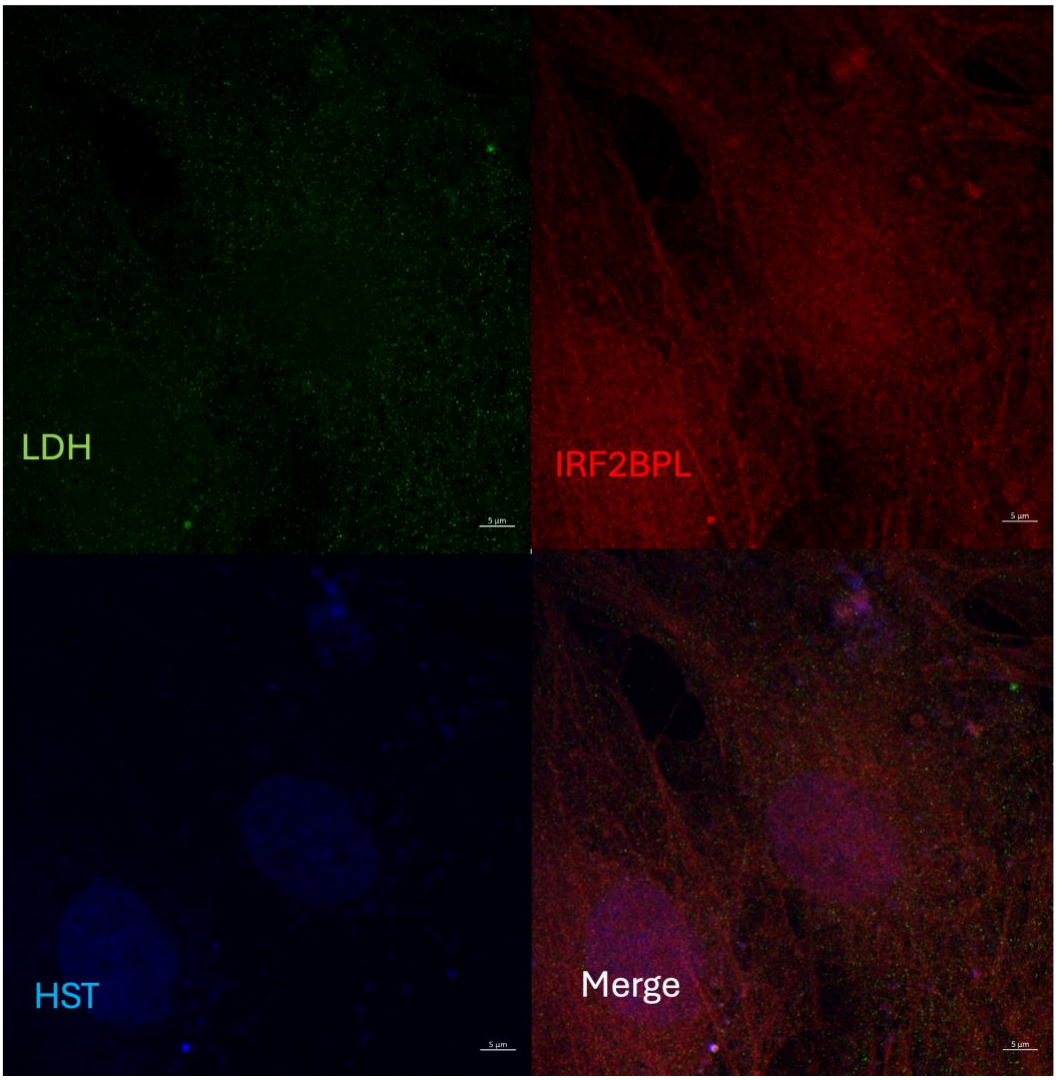

C

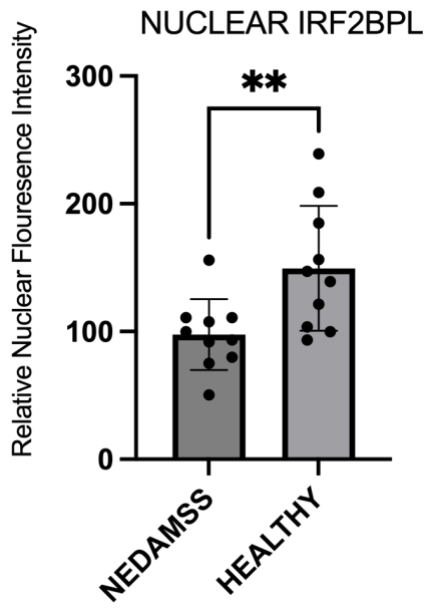

Figure 6: Immunohistochemistry of Patient and Healthy Fibroblasts Shows Differential Localization of IRF2BPL

A) NEDAMSS (PT) Fibroblast cells were fixed and imaged using confocal microscopy. The fixed cells were probed with LDH (green), IRF2BPL (red), and HST (blue). B) Healthy (AIDHC-SC1) Fibroblast cells were fixed and imaged using confocal microscopy. The fixed cells were probed with LDH (green), IRF2BPL (red), and HST (blue) All cell lines were imaged in triplicate at 63X, scale bar= 5µm representative images shown C) Quantification of nuclear IRF2BPL expression taken from triplicate of each cell line and shown as mean ± standard deviation. ns-P>.05,*-P≤0.05,**-P≤0.01,***-P≤0.001

3.3 Cells with Mutated IRF2BPL Show Variable Differences in WNT Signaling Components and Activity.

β-catenin is a common marker used to study WNT signaling as it is a key downstream component of the pathway(Liu et al., 2022). If WNT signaling was being significantly impacted in NEDMASS cells compared to the healthy controls, there would likely be a difference in *β-cat* mRNA expression. *β-cat* mRNA levels were not significantly different between the NEDAMSS and control groups (Figure 7A). This lack of difference was consistent across male and female cell lines. *LEF1* is a downstream marker of WNT signaling, which binds catenin to the DNA in the nucleus. There is a significant difference between the *LEF1* RNA expression in the NEDAMSS vs control cells (Figure 7B). *Jagged1* is involved in the WNT signaling pathway by acting as a binding ligand for the Notch delta receptor to activate the notch delta signaling (Jaleco et al., 2001). *Jagged1* mRNA expression was significantly higher in NEDAMSS cells than in controls (Figure 7C).

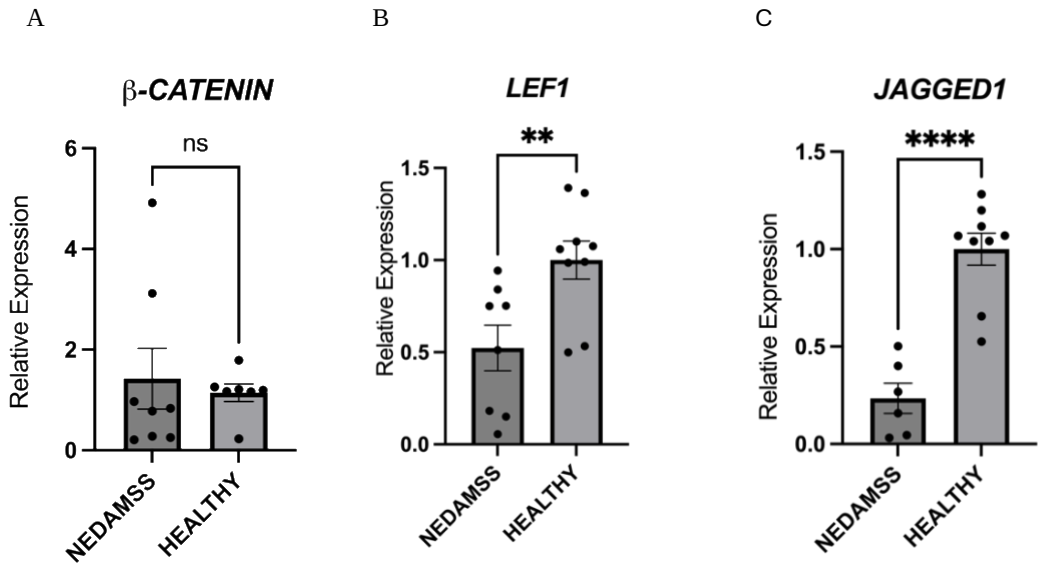

Figure 7: RNA Analysis of Select WNT Signaling Components

Relative RNA expression of *β-catenin, LEF1, and Jagged 1* in NEDAMSS and healthy cells. A cDNA library was generated from isolated mRNA and amplified via PCR. Each dot is the average of a triplicate of a cell line. This expression is relative to the geometric mean of three reference transcripts (*GAPDH, RPL0, β-Actin*). ns-P>.05,*-P≤0.05,**-P≤0.01,***-P≤0.001

Studying the expression of downstream components can indicate an increase or decrease in signaling activity, but it does not actually show the activity. By using a luciferase-based assay such as the TopFlash/FopFlash assay (Korinek et al., 1997), we observed no significant differences in WNT signaling activity between control and NEDAMSS fibroblasts (Figure 8).

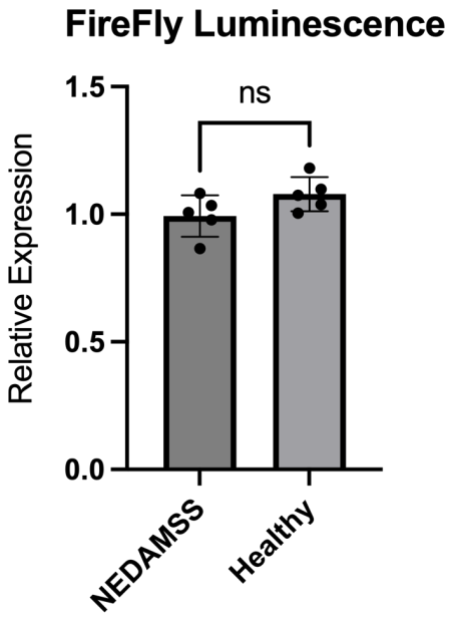

Figure 8: Luciferase Assay Shows No Significant Difference in WNT Signaling Activity in NEDAMSS Cells

Male patient and control fibroblasts were co-transfected with TopFlash (Wildtype) or FopFlash(Mutant binding sites), as well as the control vector pRL-TK for normalization. These cells were then assayed for luciferase expression. Calculations were done by dividing the luminance of the TopFlash and FopFlash treated samples by the luminescence of the control vector treated cells. Experiments were done in triplicate with the average for each cell line shown. Data was expressed as mean ± and standard deviation. ns-P>.05,*-P≤0.05,**-P≤0.01,***-P≤0.001

3.4 Analysis of AR Signaling in NEDAMSS Patient Cells

There is a lack of significant difference in RNA expression of *AR* itself in both male and female NEDAMSS cells (Figure 9A). Therefore, any impact IRF2BPL is having on AR signaling is likely happening later in the signaling pathway as opposed to diseases where there are fewer receptors (such as Spinal and Bulbar Muscular Atrophy (SBMA)). There appear to be no sex differences in the expression. There was a

significant decrease seen in the expression of *RAB25*, which has been shown to regulate cell proliferation and survival (Wang et al., 2017)(Figure 9B). Other AR-regulated genes like [LIST EACH OF THEM} show no significant differences in expression (Figures 9C-9H).

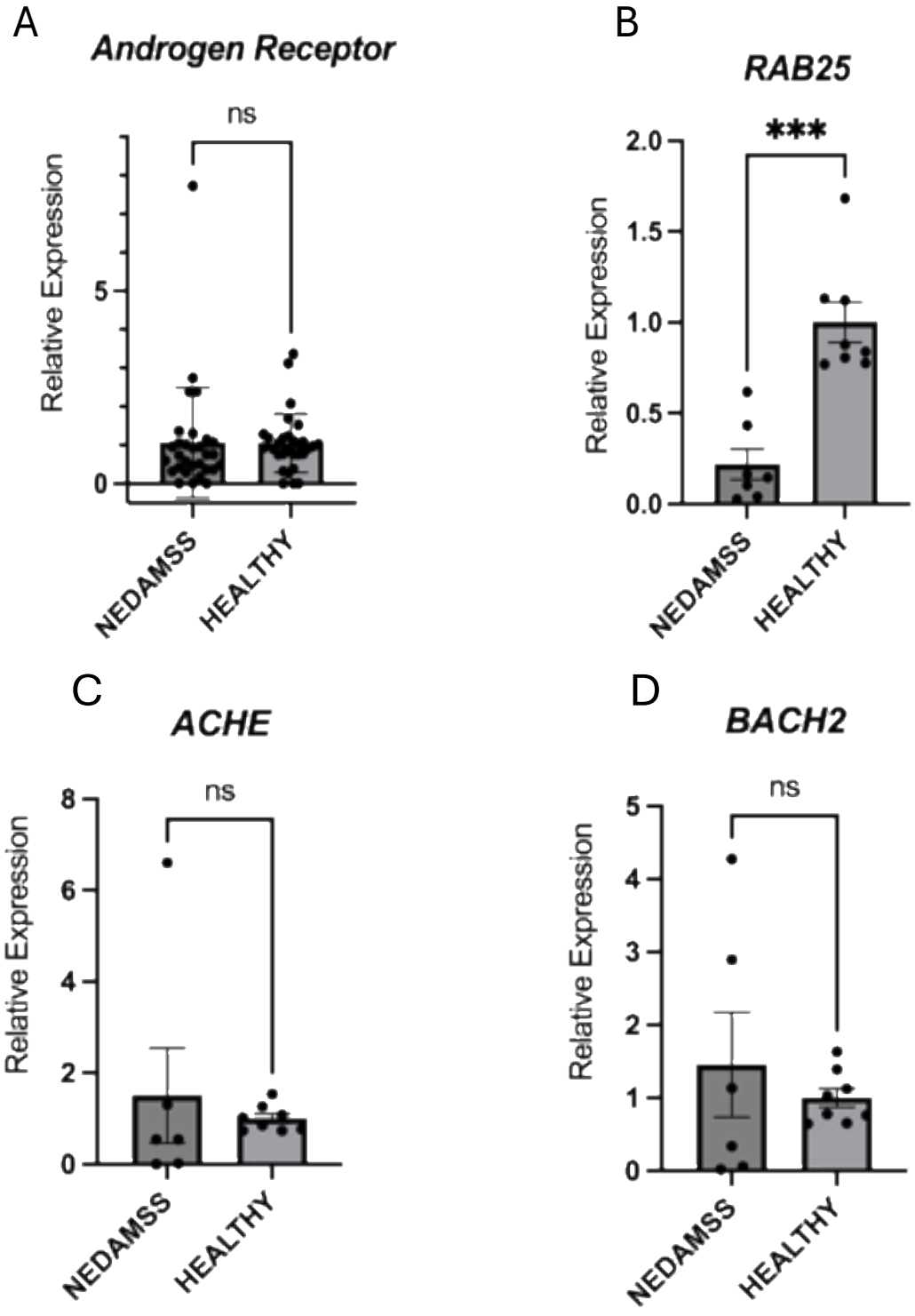
A
Androgen Receptor
ns
Relative Expression
5
0
NEDAMSS
HEALTHY
B
RAB25
***
2.0
1.5
1.0
0.5
0.0
Relative Expression
NEDAMSS
HEALTHY
C
ACHE
ns
8
6
4
2
0
Relative Expression
NEDAMSS
HEALTHY
D
BACH2
ns
5
4
3
2
1
0
Relative Expression
NEDAMSS
HEALTHY

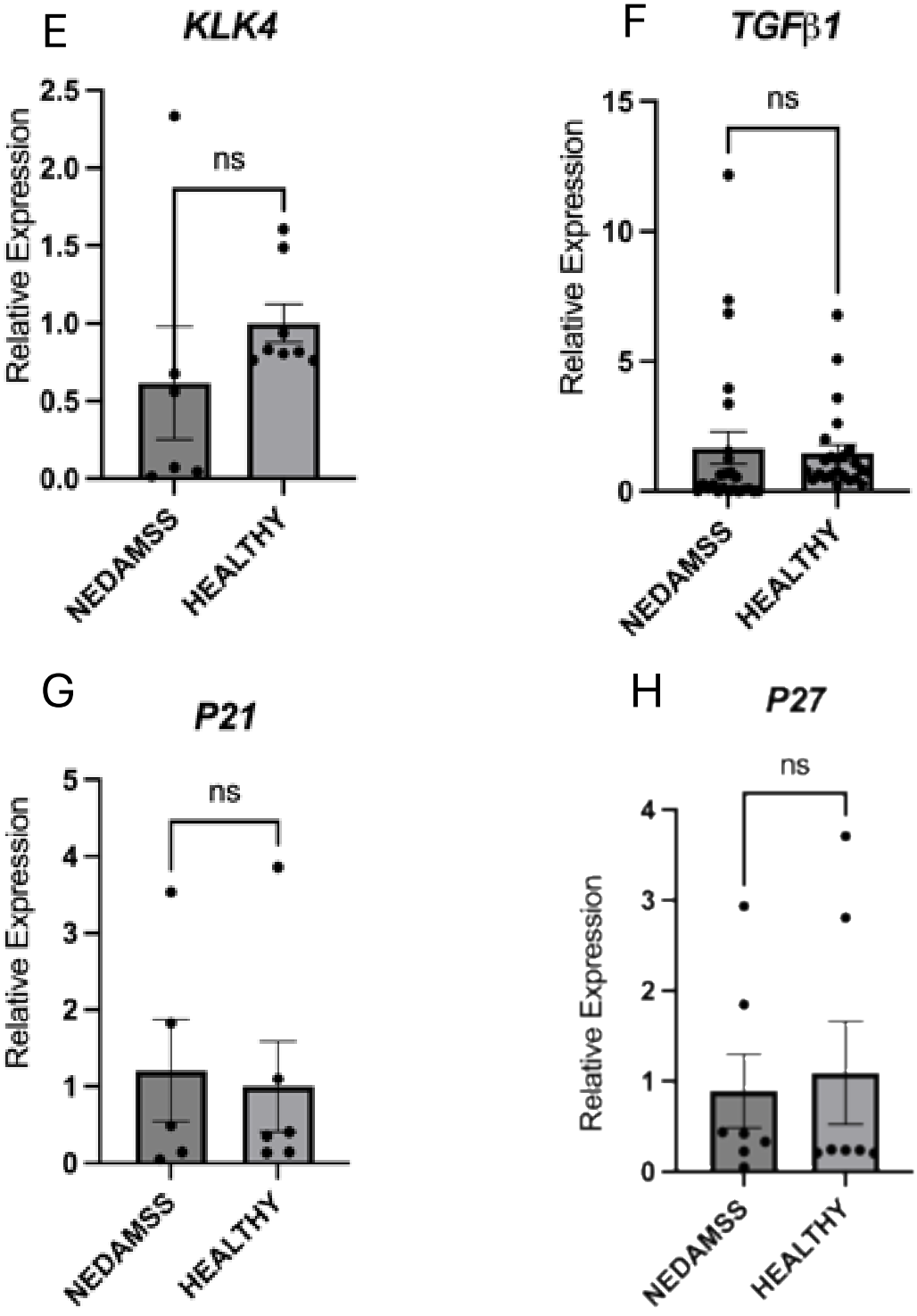
E
KLK4
Relative Expression
2.5
2.0
1.5
1.0
0.5
0.0
ns
NEDAMSS
HEALTHY
F
TGFβ1
Relative Expression
15
10
5
0
ns
NEDAMSS
HEALTHY
G
P21
Relative Expression
5
4
3
2
1
0
ns
NEDAMSS
HEALTHY
H
P27
Relative Expression
4
3
2
1
0
ns
NEDAMSS
HEALTHY

Figure 9 Relative RNA Expression of Androgen Receptor (AR) and Several Downstream Targets of AR signaling

Relative RNA expression of several AR signaling markers in Patient and healthy cells. A cDNA library was generated from isolated mRNA and amplified via PCR. The resulting cDNA was analyzed using qPCR to monitor the relative expression of the RNA transcripts of interest. Target transcript levels are relative to the geometric mean of three reference transcripts (*GAPDH*, *RPL0*, □*-actin*). A) Relative expression of *AR* RNA across triplicate of all cell lines. B) Relative expression of *RAB25,* which is significantly different between healthy and patient cells. An average of 3 replicates for each cell line is shown. C-H) relative expression of AR markers, which were not significantly different. Average of 3 replicates for each cell line shown NS-P>.05,*-P≤0.05,**-P≤0.01,***-P≤0.001

3.5 Direct Reprogramming of NEDAMSS Fibroblasts into Motor Neurons

Following direct reprogramming into motor neurons, fibroblasts were stained with two neuron-specific factors to confirm the reprogramming was successful. HB9 is a motor neuron-specific immunohistochemical marker for motor neurons(Letchuman et al., 2022). Choline acetyltransferase, a protein found only in cholinergic neurons, is an immunohistochemical marker for mature motor neurons(Granger et al., 2020). The NEDAMSS and control reprogrammed cells showed both factors (Figure 10), indicating that they were successfully transformed into motor neurons. The cells were also immunostained for Enhanced Green Fluorescent Protein (EGFP) as the lentivirus we used to transfect the cells carried a plasmid containing GFP; this was used as a way to confirm the transfection while culturing cells and treating with IN and MN media prior to fixing.

To demonstrate that these observations are not the result of the differentiation factors alone, fibroblasts from the same cell lines were plated on coverslips with the same coating as the reprogrammed cells and were given the same media and treatment, excluding the actual transfection. These cells were stained for HB9 as well as fibroblast marker fibronectin (TE7)(Sulaiman et al., 2023) (Figure 11) and were positive for TE7 and negative for HB9, confirming that they were still fibroblasts and

the HB9 signal seen in reprogrammed cells was not due to the plating method or the media.

A

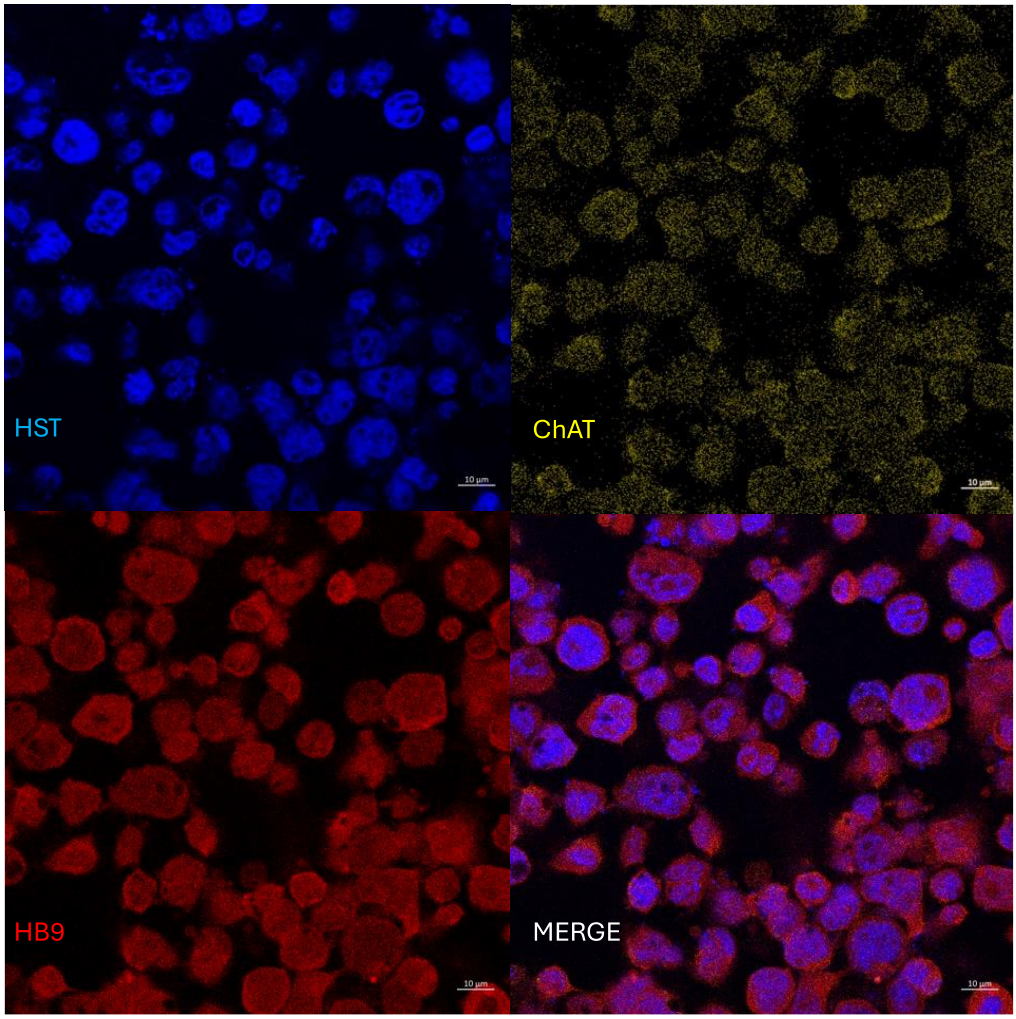

B

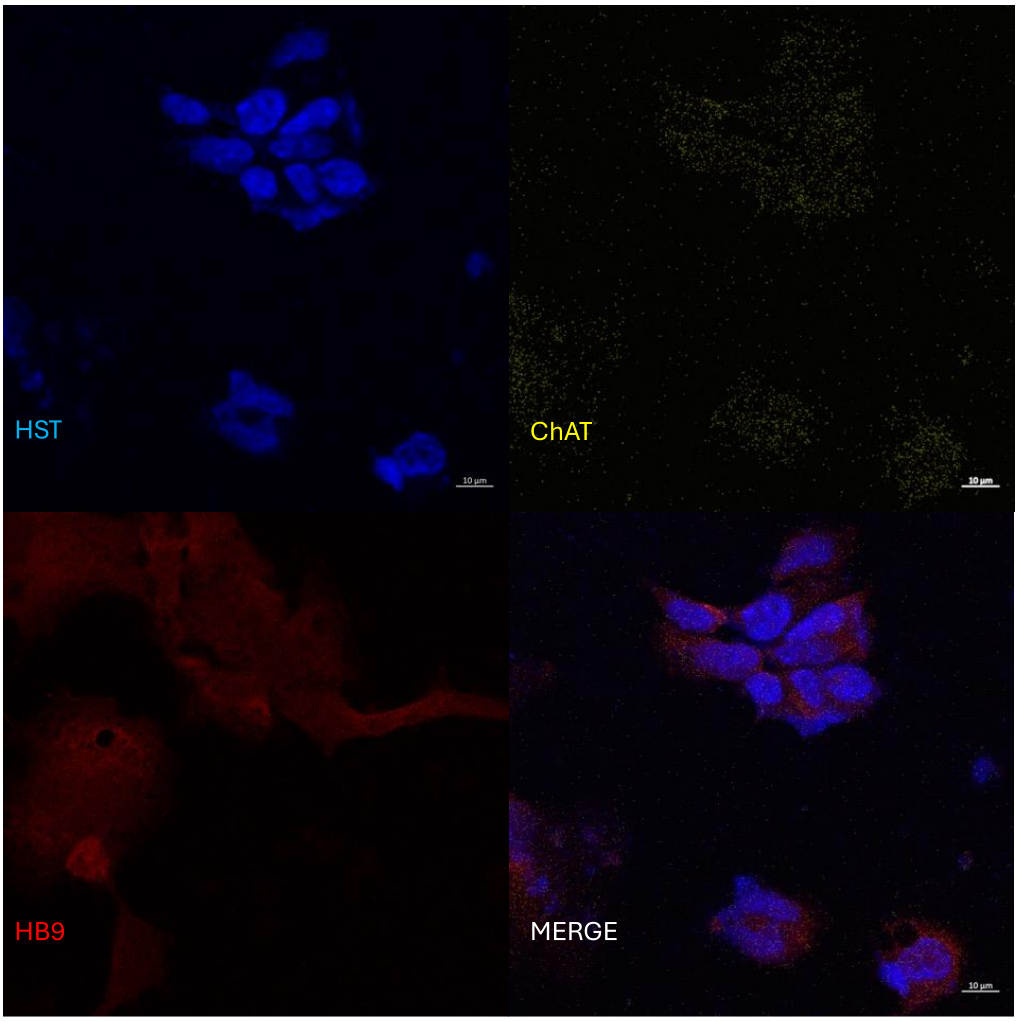

Figure 10: Patient and Healthy Fibroblasts Reprogrammed into Motor Neurons Show Two Neuron-Specific Factors.

A) NEDAMSS (UKE-672479) Fibroblast cells were fixed and imaged using confocal microscopy. The fixed cells were probed with HB9 (red), ChAT (Yellow), and HST (Blue). Cells were imaged at. 63x in triplicate, scale bar=10 µm with representative images shown B) Healthy (AIDHC-NMC5) Fibroblast cells were fixed and imaged using confocal microscopy. The fixed cells were probed with HB9 (red), ChAT (Yellow), and HST (Blue). Cells were imaged at. 63x in triplicate , scale bar=10 µm with representative images shown

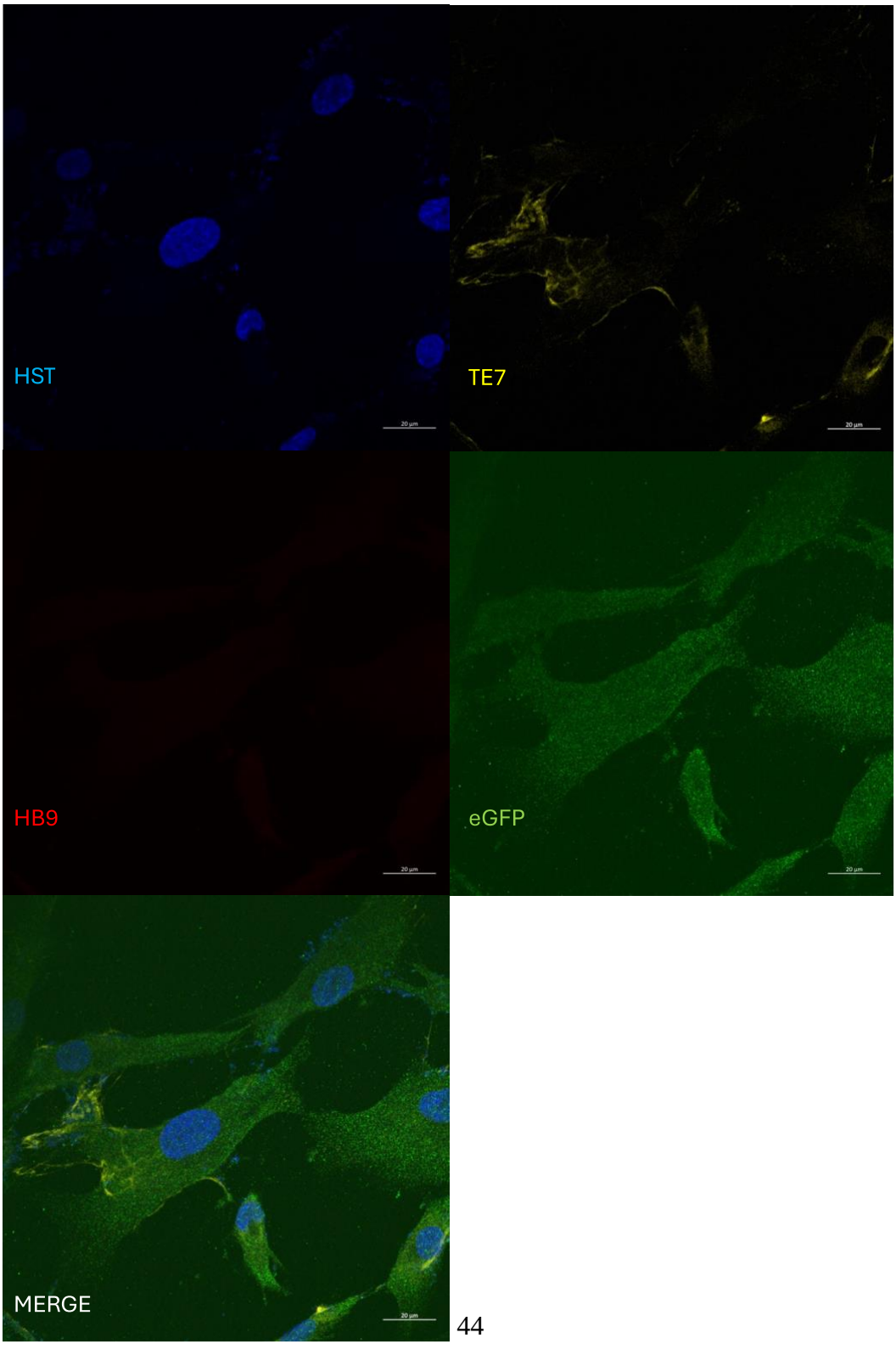
HST
TE7
HB9
eGFP
MERGE

Figure 11: Untransduced Control Fibroblasts show TE7, but no HB9

Fibroblasts were given the same treatment and processing as the reprogrammed cells above minus the transfection. These cells were fixed and imaged using confocal microscopy. The fixed cells were probed with antibodies for eGFP (green), HB9 (red), TE7 (Yellow) and HST (Blue). Cells were imaged at 63x in triplicate, scale bar=20 μm with representative images shown.

Chapter 4
DISCUSSION

Pediatric neurological disorders have one of the highest burdens of disease globally; the number of patients presenting with neurological symptoms annually has risen steadily and continues to escalate (Newton, 2018; Steinmetz et al., 2024). As the global impact of neurological diseases, especially pediatric ones, increases, there is a clear need for a better understanding of the mechanisms and pathology of these illnesses. As medicine has advanced there has been increasing pressure to look into individualized medicine. Studies have shown that not all patients with the same disease or even the same symptoms will respond equally to a given treatment. This need to personalize medicine rather than trial and error the known solutions to see what works for a particular patient means research methods need to evolve alongside this clinical understanding.

In this study, we examined what molecular phenotype, if any, is present in human cells isolated from patients diagnosed with NEDAMSS. We found that the nuclear protein IRF2BPL was mislocalized to the cytoplasm in NEDAMSS cells, confirming what has been seen previously in animal model systems like fruit flies and zebrafish(Sinha Ray et al., 2022). Interestingly, we found an increased expression of IRF2BPL in patient fibroblasts, which has not been previously reported. This was a surprising result given that many groups have hypothesized that NEDAMSS is being caused by haploinsufficiency which would be predicted to reduce IRF2BPL protein levels.

Future studies will measure how much of the expression we are seeing is from full-length IRF2BPL and how much is from the truncated varieties, developing antibodies which are specific to the N-terminus of the protein, or using in situ hybridization to discern which proteins are which. .

We found there was no significant difference in β-catenin expression which is a commonly used marker for WNT signaling misregulation (Pai et al., 2017)as well as no change WNT signaling and that any impact these mutations have on WNT signaling is happening further downstream. Previous work has focused heavily on WNT signaling, but our luciferase-based reporter assay shows no change in WNT signaling activity. While β-catenin levels were not changed, there was a significant reduction in both *LEF1* and *JAGGED1* transcripts. It is possible that any change in WNT signaling may be either a result of aberrant binding in the nucleus or a consequence of Notch-Delta signaling misregulation.

As the rat ortholog of IRF2BPL (EAP1) has been implicated as a regulator of AR signaling(Yokoyama et al., 2021), we wanted to see if there was a change in AR signaling markers in our patient samples. We found there was no significant difference in the expression of the AR but that there was a significant loss of *RAB25* transcript levels, an AR target gene. These results suggest that there may be misregulation of AR activity in NEDAMSS cells.

Human disease research is often time-consuming and costly as there is a large gap to span when translating evidence found in model organisms back into human patients. In this study, we successfully converted fibroblasts from patient and healthy controls

into motor neurons. This was confirmed by staining the reprogrammed cells for cholinergic neuron-specific factors as well as motor neuron-specific factors. As reprogramming each batch of cells took only two weeks, this could provide a timelier way to examine human neural cells. In doing the direct reprogramming, we were also able to retain the epigenetic information unique to each patient that would have been lost using a traditional stem cell-based approach. This provides a vast opportunity to explore on the cellular level what is happening in disease states in human cells. Retaining epigenetic information will lead to a broader understanding of each patient's unique disease progression. This method provides a lower cost, faster, and more direct way to examine human diseases. There is no need with this method to have costly and time-consuming animal studies, which may or may not end up finding anything applicable to humans. We are entering an age of more personalized medicine, so being able to look at the cell type of interest with a simple skin biopsy from the patient means that each patient's phenotype: genotype relationship could be studied, and doctors could reduce the use of blanket statements and theories regarding patients in large, diverse groups while ignoring each patient's individual needs.

Chapter 5
SUMMARY AND FUTURE DIRECTIONS

Neurodevelopmental disorder with regression, abnormal movement, loss of speech, and seizures (NEDAMSS) is an ultrarare degenerative neurological disease first identified in 2018. All currently identified patients have mutations in IRF2BPL, a nuclear protein whose native function remains unknown. In this study, we characterized the molecular phenotype present in cells from NEDAMSS patients and also to confirm whether the mechanisms implicated in NEDAMSS pathology in other organisms were impacted in human cells.

We confirmed the mislocalization of IRF2BPL into the cytoplasm of patient fibroblasts across 10 cell lines with different mutations. We noted a novel change in the expression of *IRF2BPL* in human fibroblasts. Across all samples regardless of mutation location. By analyzing the WNT and AR signaling cascades which have been noted as key regulators for NEDAMSS progression in model organisms(Marcogliese et al., 2022), we observed that there were no significant changes in WNT signaling activity even though markers were differentially expressed in patient cells when compared with healthy age/sex match controls. The differential expression of *JAGGED1*, *LEF1,* and *RAB25* provide good targets for further investigation of the underlying mechanisms that may be affected in NEDAMSS.

If *JAGGED1* expression is disrupted in NEDAMSS patients, this could impact Notch-Delta signaling throughout neural tissue. *JAGGED1* acts as a Notch ligand and has been shown to mitigate cell differentiation (Jaleco et al., 2001). This opens up another pathway that may be contributing to the NEDAMSS phenotype. Notch Delta signaling plays a key role in the development of the central nervous system (CNS) by mitigating cell survival and differentiation and is responsible for maintaining plasticity needed for learning and memory in adult neurons. Misregulation of Notch Delta signaling has been implicated in several diseases of the CNS (Lathia et al., 2008). Given the developmental reversal and brain atrophy seen in NEDAMSS patients and the increased cell death seen in animal models (Marcogliese et al., 2022) the misregulation of Notch could be impacting development as well as cell survival in these patients.

The reduction of *LEF1* without a change in β-catenin could indicate that the misregulation of WNT signaling seen in other organisms is a byproduct of a decreased ability to bind to DNA in the nucleus (Figure 2) rather than an increase in β-catenin itself as previously theorized. If β-catenin is not being impacted directly by these mutations, but WNT signaling is still dysregulated, it could be a result of abnormal binding of β-catenin to DNA due to the change in *LEF1* expression. The lack of difference seen in the luciferase-based assay for β-catenin dependent signaling is another point to the argument that β-catenin dependent WNT signaling is not the key mechanism behind NEDAMSS pathology.

From our study, we observed that AR itself does not have a lower expression at the RNA level, but this should be confirmed with quantification of AR protein level in NEDAMSS cells. Any change in AR signaling may be a result of misregulation further along the signaling pathway rather than at the receptor level. To elucidate, any modulation in AR signaling activity should be monitored using a luciferase-based reporter assay similar to that used for WNT signaling. Additionally, protein level analysis is needed into the function of *RAB25* in NEDAMSS cells both in relation to AR signaling and by itself as well as if there is a correlation between expression of *RAB25* and mutation location.

Now that direct reprogramming fibroblasts into motor neurons has been successfully demonstrated in healthy and patient cells, further studies into the morphology and neurite outgrowth in NEDAMSS motor neurons could provide insight into how motor neurons specifically are being affected by this disease. It would be interesting to see if the mislocalization of IRF2BPL observed in fibroblasts and other organisms is also seen in motor neurons.

Given our results regarding mislocalization and expression of IRF2BPL in NEDAMSS cells, subcellular fractionation experiments could prove insightful. Overall, there is much that is yet to be understood about NEDAMSS both on the clinical and the molecular levels. We have provided data that resolves some questions but leaves many unanswered questions that further research will address to fully characterize this disease and assist in earlier diagnosis and possible treatment options.

REFERENCES

Aas, M., Henry, C., Andreassen, O. A., Bellivier, F., Melle, I. and Etain, B. (2016). The role of childhood trauma in bipolar disorders. *Int J Bipolar Disord* **4**, 2.

Akiyama, T. (2000). Wnt/beta-catenin signaling. *Cytokine Growth Factor Rev* **11**, 273–282.

Brewer, G. J. and Torricelli, J. R. (2007). Isolation and culture of adult neurons and neurospheres. *Nature Protocols* **2**, 1490–1498.

Butchbach, M. E. R., Singh, J., Thorsteinsdóttir, M., Saieva, L., Slominski, E., Thurmond, J., Andrésson, T., Zhang, J., Edwards, J. D., Simard, L. R., et al. (2010). Effects of 2,4-diaminoquinazoline derivatives on SMN expression and phenotype in a mouse model for spinal muscular atrophy. *Hum Mol Genet* **19**, 454–467.

Cary, G. A. and La Spada, A. R. (2008). Androgen receptor function in motor neuron survival and degeneration. *Phys Med Rehabil Clin N Am* **19**, 479–494, viii.

Chen, M., Lingadahalli, S., Narwade, N., Lei, K. M. K., Liu, S., Zhao, Z., Zheng, Y., Lu, Q., Tang, A. H. N., Poon, T. C. W., et al. (2022). TRIM33 drives prostate tumor growth by stabilizing androgen receptor from Skp2-mediated degradation. *EMBO Rep* **23**, e53468.

de Carvalho, M. and Swash, M. (2023). Upper and lower motor neuron neurophysiology and motor control. *Handb Clin Neurol* **195**, 17–29.

Dull, T., Zufferey, R., Kelly, M., Mandel, R. J., Nguyen, M., Trono, D. and Naldini, L. (1998). A third-generation lentivirus vector with a conditional packaging system. *J Virol* **72**, 8463–8471.

Dupont, C., Armant, D. R. and Brenner, C. A. (2009). Epigenetics: definition, mechanisms and clinical perspective. *Semin Reprod Med* **27**, 351–357.

Granger, A. J., Wang, W., Robertson, K., El-Rifai, M., Zanello, A. F., Bistrong, K., Saunders, A., Chow, B. W., Nuñez, V., Turrero García, M., et al. (2020). Cortical ChAT+ neurons co-transmit acetylcholine and GABA in a target- and brain-region-specific manner. *eLife* **9**, e57749.

Higashimori, A., Dong, Y., Zhang, Y., Kang, W., Nakatsu, G., Ng, S. S. M., Arakawa, T., Sung, J. J. Y., Chan, F. K. L. and Yu, J. (2018). Forkhead

Box F2 Suppresses Gastric Cancer through a Novel FOXF2–IRF2BPL–β-Catenin Signaling Axis. *Cancer Research* **78**, 1643–1656.

Jaleco, A. C., Neves, H., Hooijberg, E., Gameiro, P., Clode, N., Haury, M., Henrique, D. and Parreira, L. (2001). Differential effects of Notch ligands Delta-1 and Jagged-1 in human lymphoid differentiation. *J Exp Med* **194**, 991–1002.

Jiang, X., Guan, Y., Zhao, Z., Meng, F., Wang, X., Gao, X., Liu, J., Chen, Y., Zhou, F., Zhou, S., et al. (2021). Potential Roles of the WNT Signaling Pathway in Amyotrophic Lateral Sclerosis. *Cells* **10**,.

Katzenell, S., Cabrera, J. R., North, B. J. and Leib, D. A. (2017). Isolation, Purification, and Culture of Primary Murine Sensory Neurons. *Methods Mol Biol* **1656**, 229–251.

Köhler, S., Vasilevsky, N. A., Engelstad, M., Foster, E., McMurry, J., Aymé, S., Baynam, G., Bello, S. M., Boerkoel, C. F., Boycott, K. M., et al. (2017). The Human Phenotype Ontology in 2017. *Nucleic Acids Res* **45**, D865–D876.

Korinek, V., Barker, N., Morin, P. J., van Wichen, D., de Weger, R., Kinzler, K. W., Vogelstein, B. and Clevers, H. (1997). Constitutive transcriptional activation by a beta-catenin-Tcf complex in APC-/- colon carcinoma. *Science* **275**, 1784–1787.

Kretzschmar, K., Cottle, D. L., Schweiger, P. J. and Watt, F. M. (2015). The Androgen Receptor Antagonizes Wnt/β-Catenin Signaling in Epidermal Stem Cells. *Journal of Investigative Dermatology* **135**, 2753–2763.

Lally, C., Jones, C., Farwell, W., Reyna, S. P., Cook, S. F. and Flanders, W. D. (2017). Indirect estimation of the prevalence of spinal muscular atrophy Type I, II, and III in the United States. *Orphanet J Rare Dis* **12**, 175.

Lathia, J. D., Mattson, M. P. and Cheng, A. (2008). Notch: from neural development to neurological disorders. *J Neurochem* **107**, 1471–1481.

Lescouzères, L. and Bomont, P. (2020). E3 Ubiquitin Ligases in Neurological Diseases: Focus on Gigaxonin and Autophagy. *Front Physiol* **11**, 1022.

Letchuman, S., Tucker, A., Miranda, D., Adkins, R. L., Aceves, M., Dietz, V., Jagrit, V., Leonards, A., Lee, Y. I. and Dulin, J. N. (2022). Transcription Factor Hb9 Is Expressed in Glial Cell Lineages in the Developing Mouse Spinal Cord. *eNeuro* **9**, ENEURO.0214-22.2022.

Li, B., Lu, W. and Chen, Z. (2014). Regulation of Androgen Receptor by E3 Ubiquitin Ligases: for More or Less. *Receptors Clin Investig* **1**,.

Liu, M.-L., Zang, T. and Zhang, C.-L. (2016). Direct Lineage Reprogramming Reveals Disease-Specific Phenotypes of Motor Neurons from Human ALS Patients. *Cell Reports* **14**, 115–128.

Liu, J., Xiao, Q., Xiao, J., Niu, C., Li, Y., Zhang, X., Zhou, Z., Shu, G. and Yin, G. (2022). Wnt/β-catenin signalling: function, biological mechanisms, and therapeutic opportunities. *Signal Transduction and Targeted Therapy* **7**, 3.

Loddick, S. A., Ross, S. J., Thomason, A. G., Robinson, D. M., Walker, G. E., Dunkley, T. P. J., Brave, S. R., Broadbent, N., Stratton, N. C., Trueman, D., et al. (2013). AZD3514: a small molecule that modulates androgen receptor signaling and function in vitro and in vivo. *Mol Cancer Ther* **12**, 1715–1727.

Lutterbach, B. and Hiebert, S. W. (2000). Role of the transcription factor AML-1 in acute leukemia and hematopoietic differentiation. *Gene* **245**, 223–235.

Maeda, M., Harris, A. W., Kingham, B. F., Lumpkin, C. J., Opdenaker, L. M., McCahan, S. M., Wang, W. and Butchbach, M. E. R. (2014). Transcriptome Profiling of Spinal Muscular Atrophy Motor Neurons Derived from Mouse Embryonic Stem Cells. *PLoS ONE* **9**, e106818.

Magavi, S. S., Leavitt, B. R. and Macklis, J. D. (2000). Induction of neurogenesis in the neocortex of adult mice. *Nature* **405**, 951–955.

Marcogliese, P. C., Shashi, V., Spillmann, R. C., Stong, N., Rosenfeld, J. A., Koenig, M. K., Martínez-Agosto, J. A., Herzog, M., Chen, A. H., Dickson, P. I., et al. (2018). IRF2BPL Is Associated with Neurological Phenotypes. *The American Journal of Human Genetics* **103**, 245–260.

Marcogliese, P. C., Dutta, D., Ray, S. S., Dang, N. D. P., Zuo, Z., Wang, Y., Lu, D., Fazal, F., Ravenscroft, T. A., Chung, H., et al. (2022). Loss of IRF2BPL impairs neuronal maintenance through excess Wnt signaling. *Sci. Adv.* **8**, eabl5613.

Newton, C. R. (2018). Global Burden of Pediatric Neurological Disorders. *Semin Pediatr Neurol* **27**, 10–15.

Ng, L. F., Kaur, P., Bunnag, N., Suresh, J., Sung, I. C. H., Tan, Q. H., Gruber, J. and Tolwinski, N. S. (2019). WNT Signaling in Disease. *Cells* **8**,.

Oliva, C. A., Montecinos-Oliva, C. and Inestrosa, N. C. (2018). Chapter Three - Wnt Signaling in the Central Nervous System: New Insights in Health and Disease. In *Progress in Molecular Biology and Translational Science* (ed. Larraín, J.) and Olivares, G.), pp. 81–130. Academic Press.

Pai, S. G., Carneiro, B. A., Mota, J. M., Costa, R., Leite, C. A., Barroso-Sousa, R., Kaplan, J. B., Chae, Y. K. and Giles, F. J. (2017). Wnt/beta-catenin pathway: modulating anticancer immune response. *Journal of Hematology & Oncology* **10**, 101.

Pfaffl, M. W. (2001). A new mathematical model for relative quantification in real-time RT-PCR. *Nucleic Acids Res* **29**, e45.

Schmittgen, T. D. and Livak, K. J. (2008). Analyzing real-time PCR data by the comparative C(T) method. *Nat Protoc* **3**, 1101–1108.

Shihan, M. H., Novo, S. G., Le Marchand, S. J., Wang, Y. and Duncan, M. K. (2021). A simple method for quantitating confocal fluorescent images. *Biochemistry and Biophysics Reports* **25**, 100916.

Sinha Ray, S., Dutta, D., Dennys, C., Powers, S., Roussel, F., Lisowski, P., Glažar, P., Zhang, X., Biswas, P., Caporale, J. R., et al. (2022). Mechanisms of IRF2BPL-related disorders and identification of a potential therapeutic strategy. *Cell Reports* **41**, 111751.

Soumya, B. S., Shreenidhi, V. P., Agarwal, A., Gandhirajan, R. K., Dharmarajan, A. and Warrier, S. (2023). Unwinding the role of Wnt signaling cascade and molecular triggers of motor neuron degeneration in amyotrophic lateral sclerosis (ALS). *Cellular Signalling* **110**, 110807.

Steinmetz, J. D., Seeher, K. M., Schiess, N., Nichols, E., Cao, B., Servili, C., Cavallera, V., Cousin, E., Hagins, H., Moberg, M. E., et al. (2024). Global, regional, and national burden of disorders affecting the nervous system, 1990–2021: a systematic analysis for the Global Burden of Disease Study 2021. *The Lancet Neurology* **23**, 344–381.

Sulaiman, R., De, P., Aske, J. C., Lin, X., Dale, A., Koirala, N., Gaster, K., Espaillat, L. R., Starks, D. and Dey, N. (2023). Tumor-TME Bipartite Landscape of PD-1/PD-L1 in Endometrial Cancers. *Int J Mol Sci* **24**,.

Takahashi, K. and Yamanaka, S. (2006). Induction of pluripotent stem cells from mouse embryonic and adult fibroblast cultures by defined factors. *Cell* **126**, 663–676.

Teoh, H. L., Carey, K., Sampaio, H., Mowat, D., Roscioli, T. and Farrar, M. (2017). Inherited Paediatric Motor Neuron Disorders: Beyond Spinal Muscular Atrophy. *Neural Plasticity* **2017**, 1–22.

Tran, T. T. and Lee, K. (2022). JAG1 Intracellular Domain Enhances AR Expression and Signaling and Promotes Stem-like Properties in Prostate Cancer Cells. *Cancers (Basel)* **14**,.

Tran, F. H. and Zheng, J. J. (2017). Modulating the wnt signaling pathway with small molecules. *Protein Sci* **26**, 650–661.

Tran Mau-Them, F., Guibaud, L., Duplomb, L., Keren, B., Lindstrom, K., Marey, I., Mochel, F., van den Boogaard, M. J., Oegema, R., Nava, C., et al. (2019). De novo truncating variants in the intronless IRF2BPL are responsible for developmental epileptic encephalopathy. *Genetics in Medicine* **21**, 1008–1014.

Vandesompele, J., De Preter, K., Pattyn, F., Poppe, B., Van Roy, N., De Paepe, A. and Speleman, F. (2002). Accurate normalization of real-time quantitative RT-PCR data by geometric averaging of multiple internal control genes. *Genome Biol* **3**, RESEARCH0034.

Veeman, M. T., Slusarski, D. C., Kaykas, A., Louie, S. H. and Moon, R. T. (2003). Zebrafish prickle, a modulator of noncanonical Wnt/Fz signaling, regulates gastrulation movements. *Curr Biol* **13**, 680–685.

Venkateswaran, S., Michaud, J., Ito, Y., Geraghty, M., Lewis, E. C., Ellezam, B., Boycott, K. M., Dyment, D. A., Kernohan, K. D., and Care4Rare Canada Consortium (2024). IRF2BPL-Related Disorder, Causing Neurodevelopmental Disorder with Regression, Abnormal Movements, Loss of Speech and Seizures (NEDAMSS) Is Characterized by Pathology Consistent with DRPLA. *Movement Disorders* **39**, 2102–2109.

Wan, X., Liu, J., Lu, J.-F., Tzelepi, V., Yang, J., Starbuck, M. W., Diao, L., Wang, J., Efstathiou, E., Vazquez, E. S., et al. (2012). Activation of β-Catenin Signaling in Androgen Receptor–Negative Prostate Cancer Cells. *Clinical Cancer Research* **18**, 726–736.

Wang, S., Hu, C., Wu, F. and He, S. (2017). Rab25 GTPase: Functional roles in cancer. *Oncotarget* **8**, 64591–64599.

Xu, T., Niu, C., Zhang, X. and Dong, M. (2018). β-Ecdysterone protects SH-SY5Y cells against β-amyloid-induced apoptosis via c-Jun N-terminal kinase- and Akt-associated complementary pathways. *Lab Invest* **98**, 489–499.

Yang, Q., Zhao, J., Chen, D. and Wang, Y. (2021). E3 ubiquitin ligases: styles, structures and functions. *Mol Biomed* **2**, 23.

Yokoyama, A., Kouketsu, T., Otsubo, Y., Noro, E., Sawatsubashi, S., Shima, H., Satoh, I., Kawamura, S., Suzuki, T., Igarashi, K., et al. (2021). Identification and Functional Characterization of a Novel Androgen Receptor Coregulator, EAP1. *Journal of the Endocrine Society* **5**, bvab150.

Yuan, J. S., Wang, D. and Stewart, C. N. J. (2008). *Statistical methods for efficiency adjusted real-time PCR quantification.* Germany.